Water Research 253 (2024) 121241

Contents lists available at ScienceDirect

Water Research

journal homepage: www.elsevier.com/locate/watres

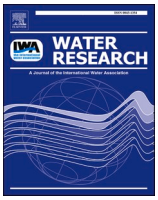

Removal of strontium by nanofiltration: Role of complexation and speciation of strontium with organic matter

Yang-Hui Cai, Akhil Gopalakrishnan, Qilin Dong, Andrea I. Schäfer *

Institute for Advanced Membrane Technology (IAMT), Karlsruhe Institute of Technology (KIT), Hermann-von-Helmholtz-Platz 1, 76344 Eggenstein-Leopoldshafen, Germany

A R T I C L E I N F O

Keywords:
Physico-chemical water treatment
flow field-flow-fractionation
cation-organic matter interaction
membrane technology
water quality
solute-solute interactions

A B S T R A C T

Strontium (Sr) removal from water is required because excessive naturally occurring Sr exposure is hazardous to human health. Climate and seasonal changes cause water quality variations, in particular quality and quantity of organic matter (OM) and pH, and such variations affect Sr removal by nanofiltration (NF). The mechanisms for such variations are not clear and thus OM complexation and speciation require attention. Sr removal by NF was investigated with emphasis on the role of OM (type and concentration) and pH (2–12) on possible removal mechanisms, specifically size and/or charge exclusion as well as solute-solute interactions. The filtration results show that the addition of various OM (10 types) and an increase of OM concentration (2–100 mgC.L^{-1}) increased Sr removal by 10-15%. The Sr-OM interaction was enhanced with increasing OM concentration, implying enhanced size exclusion via Sr-OM interaction as the main mechanism. Such interactions were quantified by asymmetric flow field-flow fractionation (FFFF) coupled with an inductively coupled plasma mass spectrometer (ICP-MS). Both extremely low and high pH increased Sr removal due to the enhanced charge exclusion and Sr-OM interactions. This work elucidated and verified the mechanism of OM and pH on Sr removal by NF membranes.

1. Introduction

1.1. Strontium in water

Both radioactive strontium (^{90}Sr) and excessive naturally occurring ^{88}Sr in water are harmful to human health (especially for infants and children) (Newcombe, 1957, Dorsey et al., 2004, Pathak et al., 2020). Internal exposure to ^{90}Sr is linked to bone and soft tissue cancer and is suspected of causing leukaemia (Newcombe, 1957, Dorsey et al., 2004, Pathak et al., 2020). Excessive exposure to ^{88}Sr may cause bone growth issues in infants and children (Dorsey et al., 2004). Both types of Sr exist as a hydrated divalent cation Sr^{2+} in most waters, and have similar physiochemical properties to calcium and barium (Suarez, 1996).

The ^{88}Sr level and distribution have been reported in natural waters ranging from 0.007–2960 mg.L^{-1} (Skougstad and Horr, 1963), depending on geographical locations, anthropogenic activities, and water body types (Health Canada 2018). The World Health Organization (WHO) and European Union (EU) have not established a guideline value for natural Sr in drinking water (World Health Organization 2017), as the monitoring of the health effects of Sr in drinking water is still ongoing (Cai et al., 2020, Khandare et al., 2020, Peng et al., 2021). The United States Environmental Protection Agency (US-EPA) included Sr in the Contaminant Candidate List 3 (CCL 3) (US-EPA 2018) in 2009 for more data collection and possibly future regulatory action (Khandare et al., 2020) and later set a Sr health reference level (HRL) of 1.5 mg.L^{-1} in 2014 (US-EPA 2014) as well as a health advisory of 4 mg.L^{-1} (based on 2 L.day^{-1} consumption of drinking water for a 70 kg adult that is not expected to cause any adverse noncarcinogenic effects for a lifetime of exposure) in 2018 (US-EPA 2018) (Table 1).

1.2. Removal of strontium and organic matter by nanofiltration

The most common Sr removal technologies include chemical precipitation (Lauchnor et al., 2013), lime-soda ash softening (O'Donnell et al., 2016), electrocoagulation (Kamaraj and Vasudevan, 2015), adsorption (Chegrouche et al., 2009, Park et al., 2021), and membrane filtration (Rana et al., 2013). Nanofiltration (NF) membranes have been increasingly applied for metal ions and organics removal due to high efficiency, simple operation and maintenance, and small footprint (Al-Rashdi et al., 2013, Oatley-Radcliffe et al., 2017).

* Corresponding author: +49 (0)721 6082 6906
E-mail address: Andrea.Iris.Schaefer@kit.edu (A.I. Schäfer).

https://doi.org/10.1016/j.watres.2024.121241
Received 18 September 2023; Received in revised form 22 January 2024; Accepted 29 January 2024
Available online 1 February 2024

Tight NF membranes (molecular weight cut-off (MWCO) of about 200 Da, such as NF90) were reported to achieve 92 to >99% Sr removal at 50 $L.m^{-2}.h^{-1}$ flux (Wadekar and Vidic, 2018); while looser NF (MWCO 300 to 500 Da), such as NF270, gave 50 to 80% removal at 85 $L.m^{-2}.h^{-1}$ flux (Chen et al., 2018). For tight NF, size exclusion is the dominant Sr removal mechanism; for loose NF, charge exclusion plays a more important role in Sr removal (Wadekar and Vidic, 2018, Schaep et al., 1998). Feedwater chemistry (ionic strength, pH, Sr concentration, and the presence of organic matter (OM)) influences the solute-solute interactions and solute-membrane interactions and hence Sr removal (Cai et al., 2020, Wadekar and Vidic, 2018, Chen et al., 2018, Chen et al., 2014).

Sr generally accumulates in surface water and groundwater in the dissolved state by the weathering and dissolution of rocks, soils, and sediments (Musgrove, 2021). The transport and removal of Sr is highly dependent on environmental factors such as competing ions (Gutierrez and Fuentes, 1991), complexing ligands such as carboxylic (Chen et al., 2018) and phenolic groups in organic compounds, carbonates and hydroxides in inorganic compounds (Felmy et al., 1998), ionic strength (Powell et al., 2015), and pH (Chen et al., 2018). OM present in water acts possess high chemical activity and can promote or impair the transport of inorganic pollutants by inducing their redox pathways (Yao et al., 2022). Dissolved OM can form soluble complexes with Cd^{2+}, Co^{2+}, Cu^{2+}, Ni^{2+}, Pb^{2+}, Zn^{2+} and other di- and trivalent cations (Borggaard et al., 2019) and influence the bioavailability and transport of As(III) and As(V) (Boussouga et al., 2021, Pothier et al., 2020), and Cr(VI) (Boussouga et al., 2023). In addition to the direct complexation with heavy metals and pollutants, OM interacts with other minerals, which enhances the migration capacity of heavy metals (Yao et al., 2022, Hu et al., 2022). Thus, organic matter deserves particular attention as this can interact in a number of ways with both Sr and nanofiltration membranes.

OM ubiquitous in waters and has very variable characteristics and functional groups, is responsible for aesthetic characteristics such as color and odor. OM contributes to the transport of pollutants and in treatment systems and plays a role in bacterial (re)growth and organic membrane fouling (Sillanpää, 2015). Due to climate change (e.g., floods and droughts) and global warming, the quantity of OM in surface waters is susceptible to rise, while the properties are bound to change (Delpla et al., 2009). The structure and characteristics of OM are also affected (e.g., more hydrophobic OM is produced), hence influencing the removal efficiency of treatment processes (Ritson et al., 2014, Lipczynska--Kochany, 2018).

The Sr removal by NF is susceptible to variable characteristics and quantity of OM. The mechanisms of OM affecting Sr removal by NF are to date not well understood and include;

i) membrane surface charge modification by OM and subsequentls enhanced Sr removal by charge repulsion (Listiarini et al., 2009, Imbrogno et al., 2018, Childress and Elimelech, 2000); and
ii) OM-Sr interactions (complexation/binding) may facilitate Sr removal via enhanced size exclusion (Chen et al., 2018).

1.3. Organic matter-strontium interaction mechanisms and factors

Numerous negatively charged OM can bind with cations (e.g., humic substances with most metal ions (Boguta and Sokołowska, 2013)) mainly due to the chemical bindings (strong form) with functional groups and the electrostatic attractive interaction (weak form) (Adusei-Gyamfi et al., 2019, Koopal et al., 2005). The most common functional groups of OM resulting in binding/complexation are carboxyl and phenolic groups (Adusei-Gyamfi et al., 2019). Based on mechanisms reported in the literature (Boguta and Sokołowska, 2013, Tipping and Hurley, 1992, Kinniburgh et al., 1996), the potential interaction mechanisms between OM and Sr^{2+} ions are summarized in Fig. 1.

Feedwater pH as well as the concentrations of cations and OM play an important role in OM-Sr interactions. These parameters determine the available binding sites, OM charge (Luo and Wan, 2013, Xu et al., 2019, Ding et al., 2015), as well as NF membrane surface charge and electrical double layer thickness (Luo and Wan, 2013). An increase in crossflow velocity or feed pressure was reported to increase Sr removal by NF due to the change in Sr concentration polarisation layer and Sr/water flux (Wadekar and Vidic, 2018, Chen et al., 2014). An increase in feed Sr concentration can enhance Sr removal, which is due to enhanced charge exclusion (interionic repulsion) (Wadekar and Vidic, 2018, Ding et al., 2015). In the absence of OM, pH values lower or higher than the NF membrane isoelectric point were reported to increase Sr removal due to the change of membrane surface charge affecting the charge exclusion (Chen et al., 2018, Ding et al., 2015). In the presence of OM, the OM-Sr interaction (speciation) and affected charge exclusion may jointly influence Sr removal. Solute-solute interactions are complicated to quantify and this will be investigated in this work in order to be able to elucidate the removal mechanisms in NF.

1.4. Quantification methods of organic matter-cations binding

Organic matter acts as organic ligands to form complexes with various metals in water (Mostofa et al., 2013). To quantify the distribution of metals among the different species formed with OM, speciation models such as the non-ideal competitive adsorption (NICA)-Donnan models can be used (Kinniburgh et al., 1999). However, the speciation results produced by such models might not be accurate for complex molecules like OM, as the total concentration of all the components and the equilibrium reaction constants are not well known (Pesavento et al., 2009). Therefore, many analytical techniques and their combinations are used for the quantification of OM-cation binding and the distribution of cations among different species. OM-cations binding can be quantified using spectroscopic techniques such as ultraviolet-visible (UV-VIS) (Baken et al., 2011, Liu et al., 2021), fluorescence (Liu et al., 2021, Xu et al., 2013), as well as size fractionation techniques such as ultrafiltration (UF) (Nifant'eva et al., 2001), electrophoresis (Keuth et al., 1998), size exclusion chromatography (Rathgeb et al., 2016, Wu et al., 2004), and flow field-flow fractionation (FFFF) (Baalousha et al., 2011, Stolpe et al., 2013, Neubauer et al., 2013, Hartland et al., 2011, Bolea et al., 2010). Hyphenated methods such as liquid chromatography with inductively coupled plasma mass spectrometry (LC–ICP-MS) have been

Table 1
Characteristics of strontium and its guideline values for drinking water.

Element	Molar mass, g. mol^{-1}	Ionic radius, nm	Hydrated radius, nm	Mobility in water, 10^{-8} $m^2.s^{-1}.V^{-1}$	Diffusion coefficient,[a] 10^{-5} cm^2s^{-1}	WHO guideline		US-EPA guideline	
						^{90}Sr, βq. L^{-1}	^{88}Sr, mg. L^{-1}	^{90}Sr, βq. L^{-1}	^{88}Sr, mg. L^{-1}
Sr	87.62	0.27	0.49	6.61	1.11–1.21	10	N/A[b]	0.3	4[c]
Ref.	(Pathak et al., 2020)	(Suarez, 1996)	(Hofer et al., 2006)	(Atkins and Paula, 2009)	(Rard and Miller, 1982)	(World Health Organization 2017)		(US-EPA 2018)	

[a] $SrCl_2$ aqueous solution at 25 °C.
[b] N/A: data not available.
[c] health advisory for a lifetime of exposure (US-EPA 2018).

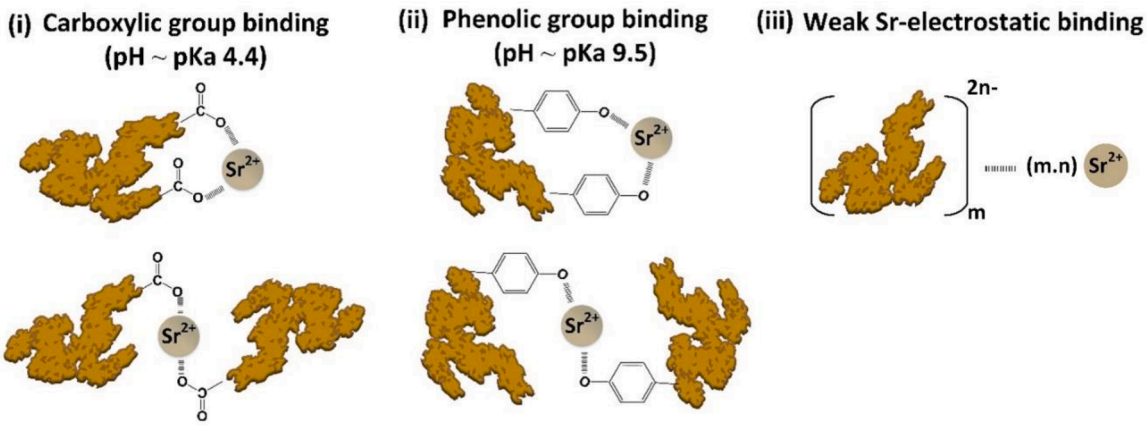

Fig. 1. Potential binding interactions between Sr^{2+} ion and OM (e.g. humic acid): (i) carboxyl group binding, (ii) phenolic group binding and (iii) weak interactions of the diffuse layer of OM with Sr^{2+} ions, adapted from (Boguta and Sokołowska, 2013; Tipping and Hurley, 1992; Kinniburgh et al., 1996).

used for characterizing organic–metal complexes in the environment (Lechtenfeld et al., 2011, Dewey et al., 2023). Size exclusion chromatography (SEC) in combination with ICP-MS has also been used to study the speciation of trace metals in water and food (Latorre et al., 2019, Rottmann and Heumann, 1994). Although very powerful in characterizing trace metal speciation in water, chromatographic systems coupled with ICP-MS often require pre-concentration of samples using solid phase extraction (Lechtenfeld et al., 2011, Boiteau et al., 2013), which limits the analysis of samples in their original state.

FFFF is a separation technique where the separation of solutes is achieved through an interaction with a force field generated by the flow of an eluent along and through a membrane. Depending on the chemical nature and size of the metal-OM complexes, FFFF can be coupled with detectors such as UV-VIS (Stolpe et al., 2013, Neubauer et al., 2013, Hartland et al., 2011, Bolea et al., 2010), fluorescence (Neubauer et al., 2013, Hartland et al., 2011), light scattering (Claveranne-Lamolère et al., 2009, Alasonati et al., 2006), total organic carbon analyzer (TOC) (Claveranne-Lamolère et al., 2009), organic carbon detector (OCD) (Moradi et al., 2020, Worms et al., 2010), and ICP-MS (Stolpe et al., 2013, Neubauer et al., 2013, Bolea et al., 2010, Alasonati et al., 2006, Worms et al., 2010, Pornwilard and Siripinyanond, 2014) to monitor metal-organic colloid interactions. FFFF-ICP-MS coupling has been investigated for the size fractionation of metal cation-OM complexes (Boussouga et al., 2021, Dublet et al., 2019, Cuss et al., 2017, Worms et al., 2019) using the change in retention of metal on complexation with OM. FFFF is suitable for a wide size range of samples and does not require pre-treatment of the sample. FFFF typically applies an ultrafiltration membrane (Kavurt et al., 2015, Bendixen et al., 2014, Kim et al., 2005, Asymmetric flow field flow fractionation 2011, Gopalakrishnan et al., 2023), while nanofiltration membrane has been shown to achieve a better separation involving smaller complexes (Neubauer et al., 2013, Dublet et al., 2019, Cuss et al., 2017, Worms et al., 2019, Li et al., 2024).

This study aims to elucidate and verify the mechanisms of OM affecting Sr removal by NF under a broad range of OM types (10), OM and Sr concentrations, and pH (2–12). The novelty of this work relies on i) the use of a broad range of OM types and 2) a coupled FFFF-ICP-MS method to quantify the OM-Sr binding interactions. The specific research questions are as follows: i) is the role of OM in Sr removal by NF dependent on OM properties? ii) which mechanisms (enhanced size exclusion or charge exclusion) is the dominant mechanism of OM affecting Sr removal by NF? and iii) which species dominate this influence on Sr removal by NF?

2. Materials and methods

2.1. Organic matter and feed solution preparation

OM types including glucose (GLU), fermented product (FP), tannic acid (TA), tannin (TANN), tea (TEA), humic acid (HA), Australian natural organic matter (AUS), worm farm extract (WF), sodium alginate (SA), and a real groundwater sample (ESI) with a large amount of natural organic matter (NOM) and salinity (Cai et al., 2020) were used to cover a broad range of OM characteristics varying size, origin, aromaticity and acidity (as shown in Table S1). Humic acid (HA, Sigma Aldrich, Germany) stock solution (about 1000 $mgC.L^{-1}$) was prepared by dissolving 2.0 g of HA and 4.0 g NaOH (Merck KGaA, Germany) in 1 L Milli-Q water and stirred (at 400 rpm) for 24 hours (Worms et al., 2010). Other organic matter (except FP and WF) were prepared by dissolving 0.5 g weight into 500 mL Milli-Q water. The original solution of 5 mL of FP and 25 mL of WF is added into 500 mL and 100 mL Milli-Q water, respectively. Some of these nine organics were not completely dissolved, such as HA, tea, and Australian NOM, which have suspended solids and unsolvable impurities. The dissolved organic carbon (DOC) fraction of these OMs was obtained by filtering the stock solutions with a 0.45 μm cellulose nitrate filter (Sartorius Co., Germany). The filtered stock solutions were stored in a cold room at 4°C and HA bottle was wrapped to prevent photolysis.

Anhydrous powder of $SrCl_2$ (^{88}Sr, ≥99.99% trace metals basis, Sigma Aldrich, Germany) was used to prepare Sr feed solutions. 10 mM NaCl (prepared from ≥99.5% powder, EMSURE®, Merck-Millipore, Germany) and 1 mM $NaHCO_3$ (prepared from ≥99.8% powder, EMSURE®, Merck-Millipore, Germany) were used as feed solution background electrolytes. The compositions of the feed solution for experiments are shown in Table S2. For OM type experiments, the DOC of each OM type in feed solution was maintained at 10 (± 0.5) $mgC.L^{-1}$ with 10 (± 0.2) $mg.L^{-1}$ $SrCl_2$, and pH was adjusted to 8.0 (± 0.1). For OM concentration experiments, 2–100 $mgC.L^{-1}$ OM (HA and FP were chosen) with 10 $mg.L^{-1}$ $SrCl_2$ was used. For Sr concentration experiments, 1–50 $mg.L^{-1}$ $SrCl_2$ with 10 $mgC.L^{-1}$ OM was used, and pH was maintained at 8.0 (± 0.1). For pH experiments, the pH range 2–12 was used for experiments (10 $mgC.L^{-1}$ OM with 10 $mg.L^{-1}$ $SrCl_2$).

2.2. Analytical methods

The Sr^{2+} concentration of samples (feed, permeate, and retentate) was measured by an inductively coupled plasma mass spectrometry (ICP-MS 7900, Agilent Technologies, USA). The UV absorbance of OM samples at 254 nm was measured by a UV-VIS spectrophotometer (Lambda 25, PerkinElmer, USA) with a one cm path length cuvette.

DOC was determined by using a TOC analyzer (Sievers M9, SUEZ, France) with acid (45% H_3PO_4) flowrate of 1 μL.min^{-1} and oxidizer (15% ammonium persulfate) flowrate of 1∼2 μL.min^{-1} to achieve the maximum oxidation efficiency. OM fractions of feed and permeate samples were characterized by liquid chromatography–organic carbon detection (LC-OCD, Model 9, DOC-Labor Dr. Huber, Germany) (Huber et al., 2011) to investigate the impact of OM fractions on Sr and OM removal. The LC-OCD system consisted of an SEC column (250 mm × 20 mm, TOYOPEARL HW50-S, Toso, Japan), UV-detector (UVD 254 nm, type S-200, Knauer, Berlin, Germany) Gräntzel thin-film UV-reactor, organic carbon detector (OCD) and organic nitrogen detector (OND, DOC-LABOR, Karlsruhe, Germany). A 22.5 mM phosphate buffer (pH 6.85) was used for sample injection and elution. A detailed system design, sample injection protocol, and analysis is described elsewhere (Huber et al., 2011, Nguyen et al., 2021).

The zeta potential (mV) of NF270 membrane with different OM types and with OM-Sr deposition was determined via streaming potential measurement using an electrokinetic analyzer (Surpass^{TM}, Anton Paar, Austria) with 10 mM NaCl as electrolyte. The electrical conductivity (EC) and pH of samples were measured by a conductivity/pH meter (model pH/Cond 3320, WTW, Germany). The calibration curves and detection limits (where relevant) of analytical equipments are summarised in Figure S7 and Figure S8.

2.3. Nanofiltration membranes and characteristics

Two commercial NF membranes, namely NF270 (FilmTec™, DuPont, USA) and HYDRACoRe 50LD (HY50, Hydranautics Nitto, USA) were used. The characteristics of the chosen NF membranes are summarised in Table 2. The FFFF requires membranes with a reasonable permeability to not exceed pressure limitations and to enable adequate force field manipulation for separation.

NF270 has a higher permeability, less negative charge, and less hydrophobic surface compared to HY50. The zeta potential of both membranes as a function of pH is shown in Figure S9. These NF membranes were chosen to investigate how a wide range of NF performance (pure water permeability of 3.5–19 L.m^{-2}.h^{-1}.bar^{-1} and salt retention of 35–45 %) and characteristics affect Sr removal.

2.4. Stirred cell filtration system and filtration protocol

A stainless-steel stirred cell system (capacity 900 mL) was used for the filtration experiments with dead-end mode, as it offers a controlled environment to investigate the impact of Sr-OM interactions on Sr removal using NF (Neale and Schäfer, 2012). The active membrane area is 38.5 cm^2, and the filtration process is driven by the pressure from 9.6 (± 0.1) bar synthetic compressed air on the top of the cell. The cell was cooled with stainless-steel loops that were connected to a chiller to maintain the feed solution temperature of 25 (± 1) °C during experiments (Fig. 2).

The detailed filtration protocol is described in Table S3, and the hydrodynamic characterization has been published previously (Imbrogno et al., 2018). The protocol included: i) membrane soaking with 10 mM NaCl for 1 hour; ii) membrane compaction for 1 hour (9.6 bar) and pure water flux measurement; iii) Sr with OM filtration experiment (constant pressure 9.6 bar, 400 mL feed, 60% recovery); iv) system cleaning with 0.01 M NaOH solution (pH 11), plenty of tap water and Milli-Q water. A recovery of 60% was used in stirred cell filtration experiments, allowing to obtain a stable Sr removal performance and to collect sufficient permeate samples for further analysis (Imbrogno et al., 2018).

2.5. Quantification of organic matter-strontium binding

The flow field-flow fractionation (FFFF) system (AF2000 Multiflow FFF system, Postnova, Landsberg, Germany) consisted of a trapezoidal channel with an active membrane area of 33.4 cm^2. To quantify the Sr concentration and Sr-OM binding, the FFFF system with a UV-VIS (PN3212, Postnova, Germany) detector was coupled with ICP-MS (Agilent, model J8403A 7900 ICP-MS, Japan) as shown in Figure S2. A polyester-based spacer of nominal thickness 500 μm was pressed on the top of the membrane coupon to create the channel. The channel was placed in a thermostat (PN4020, Postnova, Germany) at 25°C to minimize the errors associated with the fluctuations in temperature.

NF270 membranes were used in the FFFF channel. Membrane conditioning and membrane compaction were performed as described in detail in Table S4. The flow rates required for a high fractionation in the sample runs were tested for a range of flow rates (Figure S3), and the optimized sample run method is presented in Table S4. The sample injection flow rate was 0.5 mL.min^{-1}, and the elution was performed at a permeate flow rate of 2.0 mL.min^{-1} (linear gradient from 2.0 to 0 mL min^{-1} in 20 min) and a concentrate flow rate of 0.5 mL.min^{-1}. A 1 mM phosphate buffer of pH 6.6 (± 0.2) was used as the mobile phase. A low ionic strength mobile phase was used to minimize any possible interference of the mobile phase on OM size distribution and for a better retention profile in FFFF (Gopalakrishnan et al., 2023). The sample injection volume was 50 μL using the auto-sampler equipped with a 100 μL injection loop in partial injection mode.

The ICP-MS signal was used to quantify Sr concentration in the samples based on calibration curves of varying Sr concentration (Figure S6). The calibration of Sr in the FFFF-ICP-MS was performed from the injections of Sr standard solutions in FFFF to the ICP-MS by bypassing the FFFF membrane channel using a polyetheretherketone (PEEK) capillary tube with an inner diameter of 0.07 in. and length of 1.5 m. A detector flow of 0.5 mL.min^{-1} was used without a focus flow or permeate flow, for calibration, following the previously reported protocol (Boussouga et al., 2023). The percentage of Sr bound to OM (Sr_{bound}%) at a given OM concentration was used to represent the extent of Sr-OM binding, as calculated using Eq. (1).

$$Sr_{bound}\% = \frac{Sr_{(c)} - Sr_{(0)}}{Sr_{(tot)}} \cdot 100 \quad (1)$$

where $Sr_{(c)}$ is the Sr-OM bound peak area, $Sr_{(tot)}$ is the total peak area of Sr in ICP-MS in the presence of an OM of concentration 'c', and $Sr_{(0)}$ is the peak area without OM. For a sample containing Sr and OM of concentration 'c', the compound peaks consisting of the void peak and the Sr-OM bound peak ($Sr(c)$) were deconvoluted to get the peak area corresponding to $Sr(c)$. The mass of Sr bound to OM was estimated from the

Table 2
Characteristics of the NF membranes used in filtration experiments.

Membrane	Active layer	MWCO (Da)	Pore radius (nm)	Isoelectric point	Pure water permeability (L.m^{-2}.h^{-1}.bar^{-1})	Contact angle (°)	EC removal[b] (%)
NF270	Semi-Aromatic piperazine-based Polyamide	150–340 (Imbrogno et al., 2018)	0.3–0.38 (Imbrogno and Schäfer, 2019)	3.5	10–19	10–16	38–42
HY50	Sulfonated Polyethersulfone	1000 (Hydranautics 2018)	-	N/A[a]	3.5–6.5	66–70	35–45

[a] N/A: negatively charge during pH 2–12, no IEP available.
[b] Conditions: 9.6 bar, 10 mM NaCl and 1 mM $NaHCO_3$, 25 ± 1 °C.

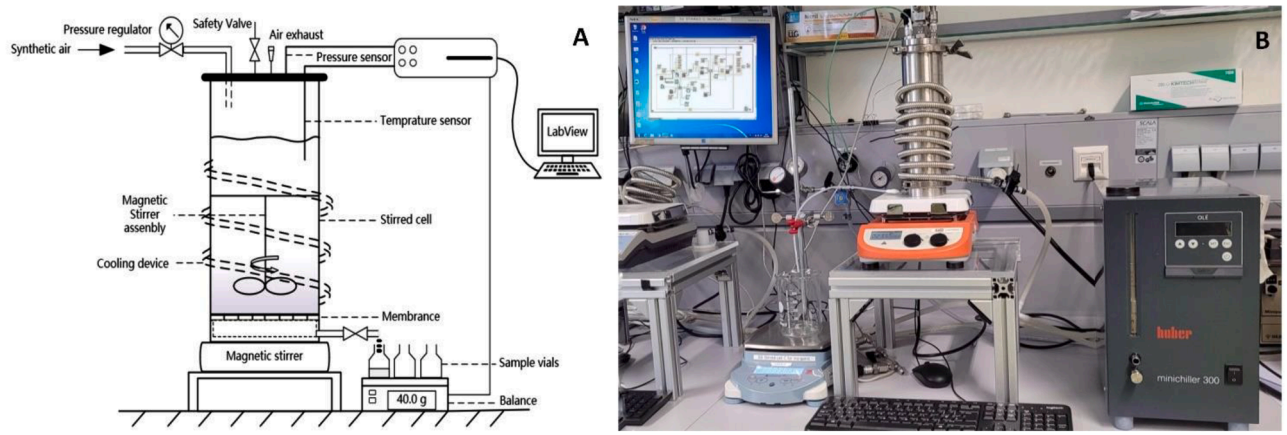

Fig. 2. Stainless steel stirred cell filtration system set-up: A) Schematic (adapted from (Imbrogno et al., 2018)) and (B) photo of the system.

Sr_{bound}% and the total injected mass of Sr. A detector flow of 0.5 mL.min^{-1} and permeate flow rate of 2.0 mL.min^{-1} (linear gradient from 2.0 to 0 mL min^{-1} in 20 min) were used for the FFFF elution. Detailed method development and optimization parameters are presented in Figure S3 and Figure S4.

2.6. Data analysis and calculations

The calculated parameters include observed retention of Sr or TOC, membrane flux, solute (namely Sr) flux, Sr concentration at the membrane surface. The calculation formulae of these parameters are summarized in Table 3.

Error analysis methods are shown in SI section 11. Since the repeated measurements of Sr and TOC concentration are not statistically significant, the absolute error of sample analysis is estimated by the maximum and minimum deviation of the measured result. To estimate the errors of calculated parameters (such as flux decline, flux recovery and deposited mass), the maximum deviation was used.

3. Results and discussion

3.1. Strontium removal by nanofiltration without organic matter

Prior to the analysis of the effect of OM on Sr removal, the Sr removal behaviors by the two NF membranes (namely NF270 and HY50) without OM were analyzed as a control experiment. Water flux, permeability, and Sr removal performance of NF membranes without OM as a function of permeate volume/recovery are presented in Fig. 3.

The steady-state flux (140 L.m^{-2}.h^{-1}) of NF270 is higher than HY50 (60 L.m^{-2}.h^{-1}) at constant feed pressure (9.6 bar) due to its higher permeability, which is in agreement with the previously reported values of 114 and 58 L.m^{-2}.h^{-1} at 9 bar for NF270 and HY50, respectively (Nair et al., 2018). HY50 has a higher MWCO than that of NF270 but with lower permeability (see Table 2), which could be attributed to the thicker active layer, low porosity, and high pore tortuosity of HY50. NF270 has a higher Sr flux (400 mg.m^{-2}.h^{-1}) than that of HY50 (240 mg.m^{-2}.h^{-1}), presumably due to its higher water flux despite the lower MWCO. NF270 has a high Sr removal (78–88%) with a lower Sr concentration in the permeate than that of HY50, while HY50 with a higher

Table 3
Calculation formula of parameters

Parameter	Unit	Formula	Eq.
Observed removal of Sr or TOC, R	%	$R(\%) = \left(1 - \frac{c_p}{c_f}\right)\cdot 100$	(1)
Water flux, J_w	L.m^{-2}.h^{-1}	$J_w = \frac{Q}{A}$	(2)
Solute (Sr) flux, J_s	mg.m^{-2}.h^{-1}	$J_S = J_w \cdot c_p$	(3)
Sr concentration at the membrane surface, c_m	mg.L^{-1}	$c_m = c_f\left((1-R) + R\cdot e^{\frac{J_v}{k_m}}\right)$	(4)
Mass transfer coefficient, k_m	m.s^{-1}	$k_m = \frac{Sh\cdot D}{d_h}$	(5)
Osmotic pressure at the membrane surface, π_m	bar	$\pi_m = \sum ic_m \cdot R\cdot T$	(6)

where:

c_p: permeate concentration, $\frac{\sum c_{i,p}V_{i,p}}{V_{tot,p}}$, mg.L^{-1} or mgC.L^{-1}; c_f: initial feed concentration, mg.L^{-1} or mgC.L^{-1};
Q: permeate flow rate, L.h^{-1}; A: effective membrane area, m^2;
J_w: water flux, L.m^2.h^{-1}; c_p: permeate concentration, mg.L^{-1};
R: observed removal; J_v: volumetric flux (m.s^{-1}) and k_m is the mass transfer coefficient (m.s^{-1});
Sh: Sherwood number, 1700; d_h hydraulic diameter, 0.007 m for this specific stirred cell, adapted from (Imbrogno and Schäfer, 2019);
D: Sr^{2+}diffusion coefficient ($0.794\cdot10^{-9}$ m^2.s^{-1}) in water at 25 °C, adapted from (Flury and Gimmi, 2002);
i: Van't Hoff factor, dimensionless; R: the ideal gas constant, 0.083 L.bar.K^{-1}.mol^{-1}; T: the absolute temperature, K, =273 + t (°C); c_m: each solute molar concentration at the membrane surface, mol.L^{-1}.

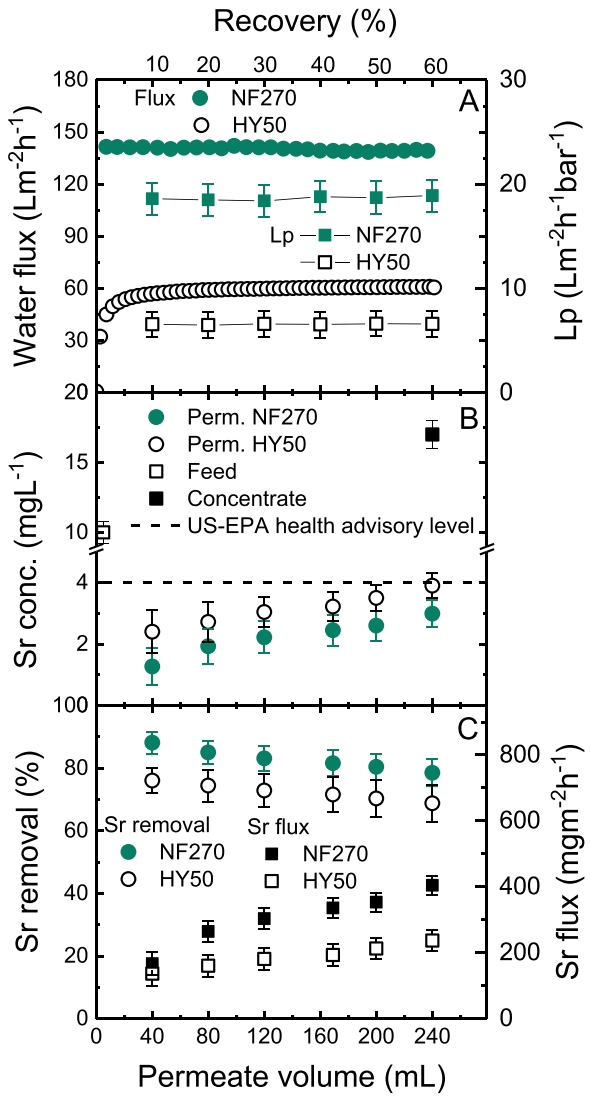

Fig. 3. NF membrane performance (A) flux and pure water permeability; (B) Sr concentration of feed, concentrate and permeate; (C) Sr removal and Sr flux as a function of permeate volume and recovery. 400 mL feed solution: 10 mg.L^{-1} $SrCl_2$, 10 mM NaCl and 1 mM $NaHCO_3$, pH 8.0 ± 0.1 and 25 ± 1 °C.

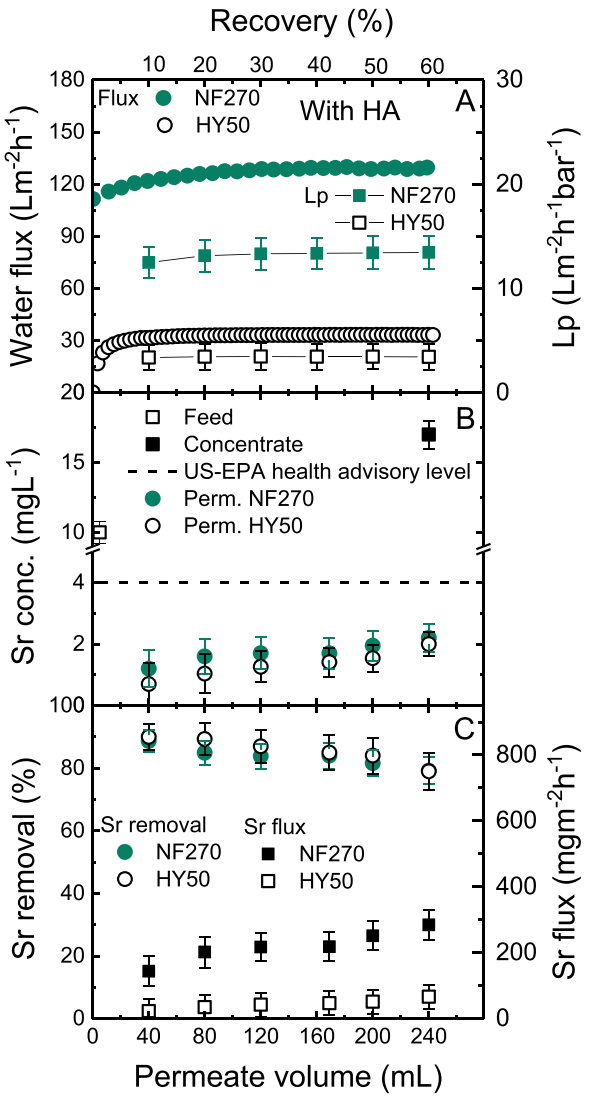

Fig. 4. NF membrane performance (A) flux and permeability; (B) Sr concentration of feed, concentrate and permeate; (C) Sr removal and Sr flux as a function of permeate volume and recovery. 400 mL feed solution: 10 mg.L^{-1} $SrCl_2$, 10 mgC.L^{-1} humic acid, 10 mM NaCl and 1 mM $NaHCO_3$, pH 8.0 ± 0.1 and 25 ± 1 °C.

MWCO has a Sr removal (69–76%) closer to that of NF270, which is probably due to charge exclusion.

The Sr removal observed for NF270 is in agreement with the previous reports of 72% removal at 5 mg.L^{-1} Sr concentration, pH 4.5 and 5 bar pressure (Chen et al., 2018). The next section will discuss how organic matter (humic acid (HA) as a typical representative of OM) affects Sr removal.

3.2. Strontium removal by nanofiltration with organic matter

Organic compounds that can form complexes with Sr are exploited for enhancing Sr retention in nanofiltration. Acid functional group bearing polymers such as polyacrylic acid has been used to improve Sr removal with NF270 and XN 45 (Chen et al., 2018), NF70 (Gaubert et al., 1997), and NF90 (Zhao et al., 2023). Organic matter naturally occurring in water may also interact with Sr and influence membrane surface charge, which consequently may affect the Sr removal by NF membranes. Thus, this section is to verify whether typical organic matter affects Sr removal performance by nanofiltration. Water flux, permeability and Sr removal performance of NF membranes with humic acid (as a typical organic matter) as a function of permeate volume/recovery are presented in Fig. 4.

In the presence of humic acid (HA), water flux decreased while the Sr removal increased for both NF membranes when compared to the absence of HA (Fig. 3). The Sr concentration in all the permeate samples was below the US-EPA health advisory level. This means the OM indeed influences the Sr removal and HA causes a positive effect of Sr removal. Sr removal by HY50 increased to a similar extent as NF270 in the presence of HA, however with much less flux/permeability than that of NF270. Previous research showed similar results, for example, a decrease in water flux and increase in metal removal was reported for Cr (III) with HY50 in presence of HA (Boussouga et al., 2023). The presence of HA and NOM may induce complex formation with Sr^{2+} (Cai et al., 2020) in a similar fashion to Cr^{3+} (Boussouga et al., 2023) and Ca^{2+} (Listiarini et al., 2009), which possibly enhanced the retention of Sr.

A variety of organic matter may interact with Sr and NF membranes differently; thus the next section will discuss whether other OM types enhance Sr removal in a similar fashion to humic acid.

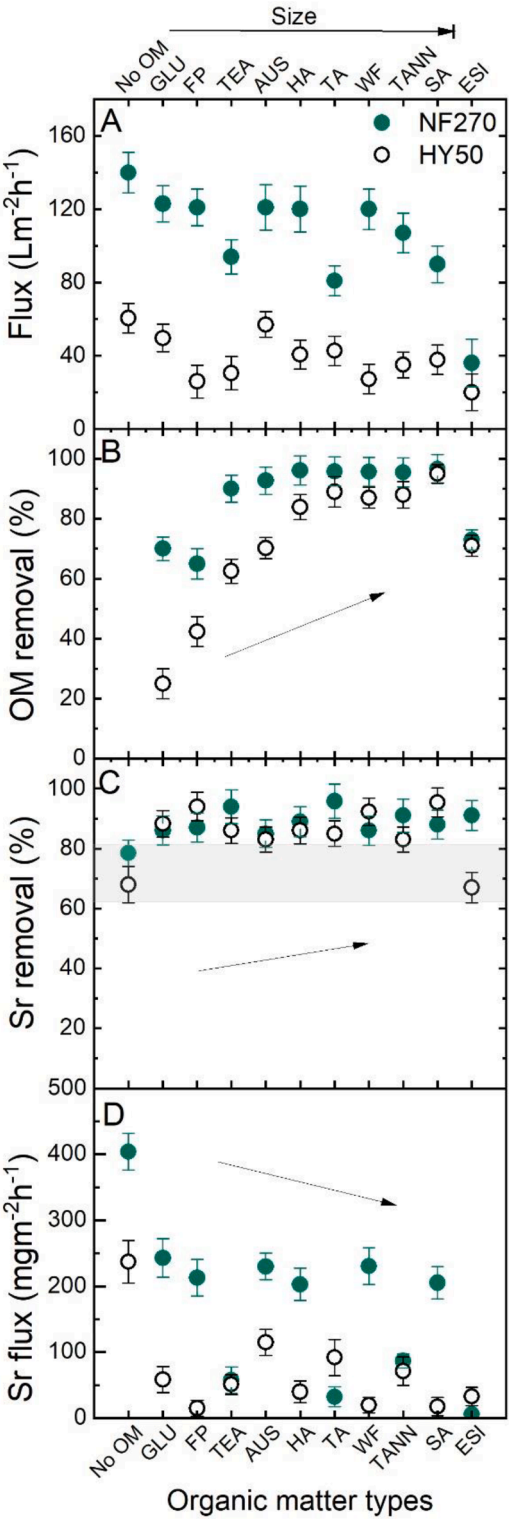

Fig. 5. (A) Steady-state flux; (B) OM retention; (C) Sr retention and (D) Sr flux as a function of OM types. Feed 10 mg.L^{-1} $SrCl_2$ with 10 mgC.L^{-1} OM, 10 mM NaCl and 1 mM $NaHCO_3$, except for the ESI real groundwater sample, 25 ± 1 °C, and pH adjusted to 8.0 ± 0.1, 60 % recovery. The grey range represents the Sr removal without OM and the dash arrows represent the trend.

3.3. Strontium removal by nanofiltration with organic matter types

To determine if the enhancement of Sr removal depends on OM matter characteristics, the membrane performance (flux, OM removal, Sr removal and Sr flux) for ten different OM types is presented in Fig. 5. The OM are presented in the increasing order of their apparent molecular weight (Nguyen et al., 2021). The molecular weight of selected OM ranges from 180 Da (GLU) to up to 180 kDa (SA) as described in Table S1. The OM removal increased with molecular weight as expected (Fig. 5B). NF270 shows higher OM removal than HY50. LC-OCD analysis of feed and permeate samples of OM (Figure S15) confirms that more low molecular weight fractions permeate through HY50 than through NF270.

The addition of various OM types increased Sr removal for both NF membranes from 69–79% (HY50) to 83–96% (NF270) (Fig. 5C). However, the change in Sr removal was not observed proportionally to the OM removal (25 to 97%) since the presence of OM (except ESI) resulted in high Sr removal (≥83%). The potential mechanisms for increased Sr removal include: i) increased retention of Sr^{2+} bound to OM molecules by NF via enhanced size exclusion (Chen et al., 2018), and ii) OM (with an inherent net negative charge) may make membrane surface more negatively charged, increasing the Sr retention via enhanced charge interaction (Listiarini et al., 2009, Shim et al., 2002, Tang et al., 2007). Low Sr removal (67%) of HY50 with real groundwater is probably due to the weakened charge exclusion, namely the HY50 membrane surface may become less negatively charged at high salinity of this real groundwater (Braghetta et al., 1997).

To verify if this enhanced Sr removal is due to charge exclusion due to modification of membrane surface charge (more negative) with different OM types, the zeta potential of NF270 and HY50 membranes with different OM types was measured as a function of pH (see Figure S9). At pH 8.0 ± 0.1, NF270 membrane surface charge (-57 mV) did not show considerable variation in the presence of Glu, FP, Tea, HA, TANN, and SA. NF270 membrane surface became less negatively charged in the presence of AUS NOM (-38 mV), TA, and WF (both -45 mV).

These results suggest that the charge interaction of Sr^{2+} with the membrane is not enhanced in the presence of OM, even though the Sr removal was enhanced. Thus, the change in membrane surface charge is probably not a major mechanism of Sr removal. On the other hand, for HY50, the zeta potential values became more negative upon exposure to various OMs. The zeta potential was changed from -21 mV for pristine HY50 to the range of -24 to -36 mV in the presence of OM. The enhancement of the negative charge of HY50 after the surface modification by OM might have contributed to the improved Sr retention of HY50 when compared to NF270. Membrane surface charge modification during the adsorption of organic matter can affect electrostatic interactions (Childress and Elimelech, 1996) which may consequently enhance the retention of Sr.

3.4. Strontium removal with increasing organic matter quantity

OM quantity in natural waters is variable with weather, season and susceptible to increase due to climate change (Delpla et al., 2009), which may enhance the OM-Sr interactions and thus Sr removal by NF. As a consequence, it is of interest how OM concentration influences Sr removal. In addition to the commonly used HA, FP was selected as model OM with NF270 membrane because the characteristics of FP are very different (Table S1) even though the Sr removal is similar. This may point at a different mechanism.

Increasing OM concentration enhanced Sr retention by NF270 from 78–80% (FP) to 83–97% (HA), reduced Sr flux, and then remained constant at high OM concentrations, probably due to the saturation of Sr-OM interactions. HA caused relatively higher Sr retention than FP at high OM concentration (Fig. 6C), which is probably due to more Sr-OM binding with HA than FP.

To verify this hypothesis, the amount of Sr bound with HA and FP was quantified using coupled FFFF-ICP-MS. Sr signals produced in FFFF-ICP-MS correspond to the Sr retained by the membrane in the channel. The presence of OM in the Sr solution leads to Sr-OM complex formation.

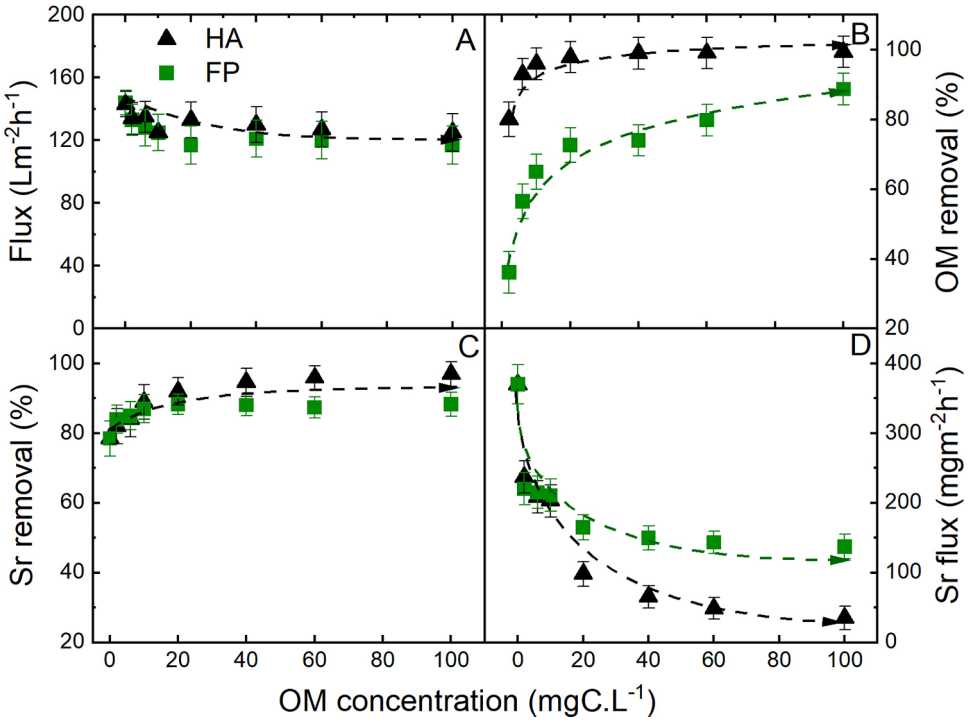

Fig. 6. (A) Steady-state flux; (B) OM removal; (C) Sr removal; and (D) Sr flux as a function of OM (HA and FP) concentration (as TOC). NF270 membrane, recovery 60 %; 10 mg.L^{-1} $SrCl_2$ with 10 mM NaCl and 1 mM $NaHCO_3$, 25 ± 1 °C, pH 8.0 ± 0.1, feed pressure 9.6 bar. The dash arrows show the trend.

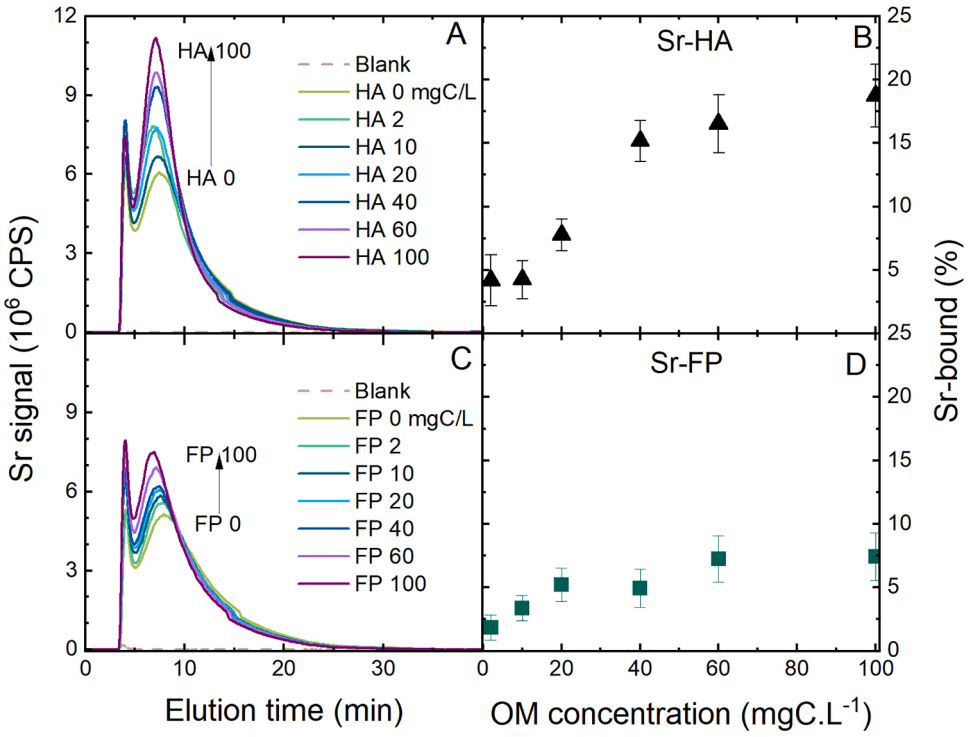

Fig. 7. Sr signal (in FFFF-ICP-MS) as a function of elution time with different concentrations of HA (A) and FP (C); Sr bound with HA (B) and FP (D) as a function of OM concentration at 10 mg.L^{-1} $SrCl_2$, NF270 membrane, Q_c 0.5 mL.min^{-1}, Q_p 2.0 mL.min^{-1} (gradient).

Sr-OM complexes that are larger than the dissolved Sr increase the Sr retention by size exclusion.

In addition to size exclusion mechanisms, Sr retention may be increased by the interaction of the Sr-OM complexes with the membrane. This means that the complexes that are retained are deposited on the membrane and modify the retention properties of these membranes. Thus by measuring the Sr signal produced in the presence and absence of OM, the Sr-OM binding was quantified using equation (1). Sr-OM mixed solutions with a Sr concentration 5.5 mg.L^{-1} and OM concentration 2–100 mg.C L^{-1} (corresponding to an OM/Sr ratio of 0.4–18.2) were

used for evaluating the Sr-OM binding. The results are presented in Fig. 7.

The Sr signal in ICP-MS increased with the increases in OM concentration implying that more Sr is retained in the presence of OM. Sr bound to the OM was calculated based on the increase in Sr peak area increase with OM using equation (1)). Sr-HA bound (%) increases with HA concentration and reaches a plateau when HA concentration approaches 100 mgC.L^{-1}. Such a breakthrough of Sr-FP bound (%) with FP concentration was not observed in the case of FP. This implies that more Sr was bound to HA than with FP at OM concentrations above 20 mgC.L^{-1}. This supports the hypothesis that the higher Sr removal observed (Fig. 6) in the presence of HA, compared to FP, is due to the higher Sr-HA binding. The higher Sr binding with HA than FP is most likely due to the difference in the nature and number of binding sites of the OM. The binding ability of an OM with Sr can be quantified in terms of the total phenolic and carboxylic acidity of the OM. The approximate ratio of total acidity of HA: FP is 4:1 (see Table S1) (Cai et al., 2022). The aromaticity of HA is 80 times higher, and the net anionic charge is about 79 times higher than that of FP (Table S1) (Cai et al., 2022). Therefore, the Sr-HA binding is potentially higher when compared to Sr-FP binding due to the interaction Sr with the acidic groups and charged sites of HA.

The FFFF-ICP-MS results of Sr-HA binding are compared with Visual MINTEQ simulation results using the NICA-Donnan model. Sr bound to HA by carboxylic acid interaction and electrostatic interaction was found to be predominant at OM concentrations $\geq$ 50 mgC.L^{-1} (Figure S10). At 10 mg.L^{-1} $SrCl_2$ and 60 mgC.L^{-1} HA, 80% Sr was bound to HA, while 20% was unbound, which increases to 91% Sr bound and 9% unbound at a HA concentration of 100 mgC.L^{-1} (Figure S11). Although there is a marginal difference between the Sr-HA bound% between the FFFF experimental and Visual MINTEQ simulation estimations, the simulation underlines that Sr binds very effectively to HA at high HA concentrations. The disparity in Sr-HA bound% between the experimental and simulation data could be due to i) binding site (carboxylic and phenolic hydroxyl groups) concentration in NICA-Donnan model is not corrected to match experimental conditions, ii) variation in Sr-HA binding equilibrium time upon performing the FFFF estimation (at short equilibrium time of 1 h) and Visual MINTEQ simulation (at complete equilibrium), iii) underestimation of Sr-HA binding in FFFF due to the dissociation of Sr from Sr-HA complex during the focusing/elution steps, iv) underestimation of Sr-HA binding in FFFF due to the loss of Sr-HA fractions via permeation through the membrane or adsorption on the membrane. A detailed examination (section 14, supporting information) of these possible factors indicates that the longer equilibrium time required before FFFF experimental analysis and

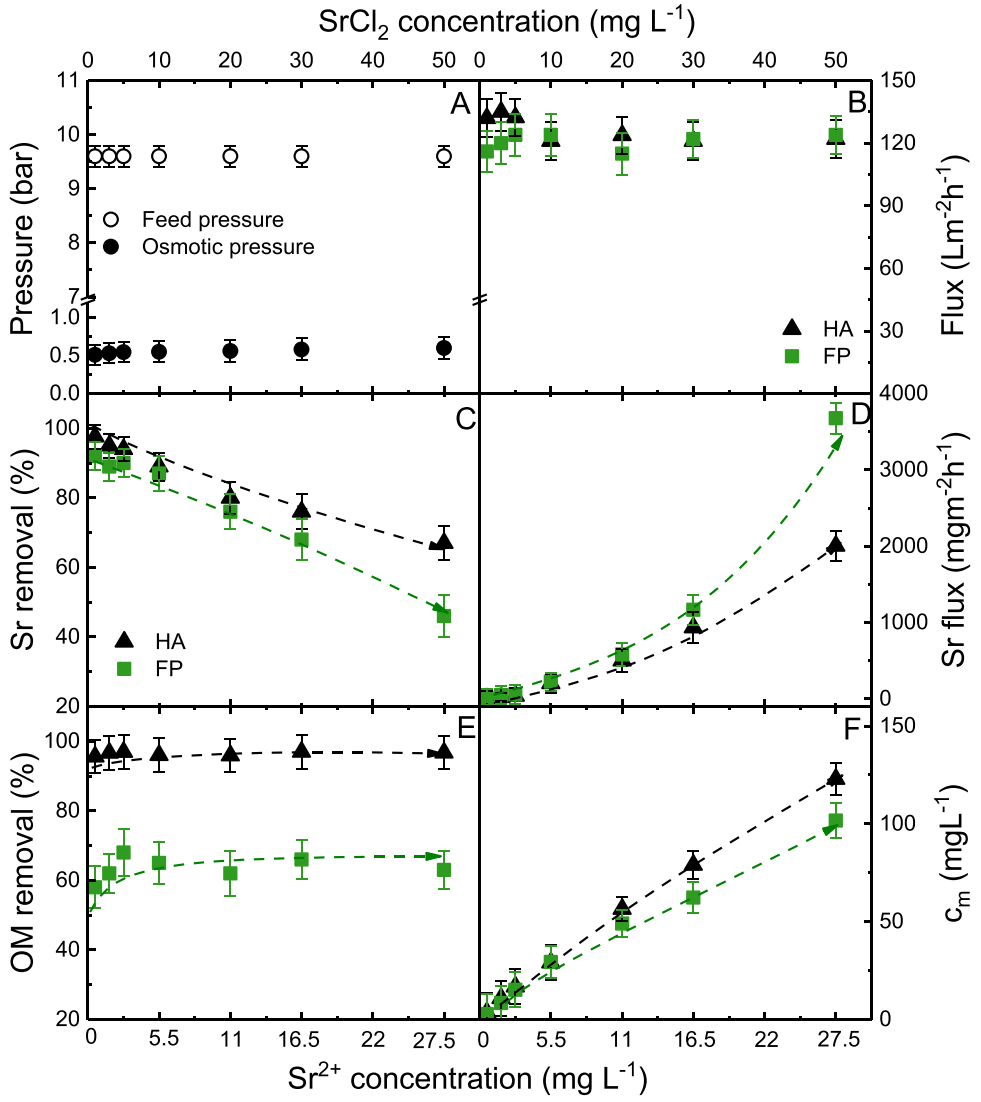

Fig. 8. (A) Feed pressure, osmotic pressure at the membrane surface; (B) membrane steady-state flux; (C) Sr removal (D) Sr flux; (E) OM removal and (F) Sr concentration at membrane surface c_m as a function of Sr concentration. NF270, 60 % recovery; 10 mgC.L^{-1} OM (HA and FP) with 10 mM NaCl and 1 mM $NaHCO_3$, 25 ± 1 °C, pH 8.0 ± 0.1.

parameter optimization in Visual MINTEQ could be the major factors contributing to the difference in the empirical and modeled data of Sr-HA binding. Visual MINTEQ simulation with the NICA-Donnan model was not performed for FP as the NICA-Donnan model consists of only humic acid and fulvic acid parameters, and the complexation constants for FP and Sr is not available.

When Sr-OM bound (%) and the Sr removal was plotted against the ratio of concentration of OM/Sr, Sr-OM binding and Sr removal were found to attain a breakthrough towards a particular OM/Sr concentration ratio for both HA and FP (Figure S14). At an OM/Sr ratio of 4 mgC.mg^{-1} for FP and 11 mgC.mg^{-1} for HA, which can be termed as 'critical OM/Sr ratio', the Sr-OM binding and Sr removal acquired a breakthrough. Above the critical OM/Sr ratio, the Sr-OM binding does not increase further, implying that all the labile Sr has undergone complexation with OM at the critical OM/Sr ratio. This breakthrough in Sr-OM binding is also observed in the Visual MINTEQ simulation where the Sr-OM bound (%) acquires a plateau at a particular HA and Sr concentration (Figure S11). NF experiments with a range of Sr concentrations were performed to evaluate if OM/Sr ratio acts as a decisive factor in Sr transport.

3.5. Strontium removal with increasing strontium concentration

Sr concentration and distribution vary in natural waters depending on the geographical locations, anthropogenic activities and water body types, which are bound to affect Sr removal of NF in presence of OM. To investigate role of OM/Sr ratio in determining the Sr transport, Sr concentration was varied in the range of 0.5-27.5 mg.L^{-1} with a fixed OM concentration of 10 mgC.L^{-1} (corresponding to an OM/Sr ratio of 18.2-0.4). Sr removal in NF and Sr-OM binding in FFFF were evaluated as a function of Sr concentration (see Fig. 8).

Increasing Sr^{2+} concentration to 27.5 mg.L^{-1} did not contribute to significant osmotic pressure increase and flux decline, but it resulted in lower Sr removal and higher Sr flux in the presence of 10 mgC.L^{-1} OM. The Sr^{2+} concentration at the membrane surface (considering CP) increased linearly with the initial Sr concentration (Fig. 8F), enhancing the Sr^{2+} diffusion through NF membranes. This could explain the reduction in Sr removal. The following hypotheses are proposed to elucidate the mechanism of higher Sr removal (66%) in presence of HA than FP (49%) at high Sr^{2+} concentration (27.5 mg.L^{-1}); i) a higher degree of Sr-HA than Sr-FP binding in solution resulting in more Sr retained with HA; ii) more deposition of Sr-HA (rather than Sr-FP) complexes on the membrane surfaces and this either facilitating adsorption of Sr^{2+} (if excess negative charges are available at Sr-HA complex deposited membrane surface) or charge exclusion of Sr^{2+} (if excess positive charges due to Sr^{2+} are available at Sr-HA complex deposited membrane surface); iii) more Sr-HA complex deposition than Sr-FP complexes alters the pore size of the membranes such that the Sr removal by steric exclusion increases. The validity of these hypotheses will now be investigated.

Sr-HA and Sr-FP binding at different Sr^{2+} concentrations were evaluated using coupled FFFF-ICP-MS (see Fig. 9) to verify the first hypothesis of whether HA-Sr binding is more than FP-Sr binding at high Sr concentration. The surface potential of the membranes (see Figure S9b) was evaluated to verify the second hypothesis of whether the surface charge variation upon deposition of the Sr-OM complexes plays a role in Sr removal. The pure water permeability of membranes after filtration with different OM (HA and FP) was compared to verify the third hypothesis. The permeability of the NF270 membrane after Sr-HA filtration was reduced to some extent, while almost no reduction after Sr-FP filtration was observed. This implies that pores blockage by Sr-HA complexes at a Sr concentration of 27.5 mg.L^{-1} was a possible contribution. This substantiates the third hypothesis that the reduction in pore size of the membrane may contribute to the Sr removal.

Surprisingly, the amount of Sr bound to OM did not vary considerably with Sr^{2+} concentration for both HA and FP. The Sr concentration range 5.5 to 27.5 mg.L^{-1} and OM concentration 10 mgC.L^{-1} corresponds to an OM/Sr ratio of 1.8 to 0.4. In this OM/Sr ratio, the quantity of Sr-OM complexes formed is perhaps too low to observe a difference in the Sr-OM bound (%) as evident from Fig. 7 and Figure S14. This is probably due to the limited number of available functional groups of OM that could bind with Sr. At such a low OM/Sr ratio, Sr^{2+} ions are in excess, and the low amount of Sr-OM complexes does not lead to an observable charge interaction or size exclusion with the membrane. The

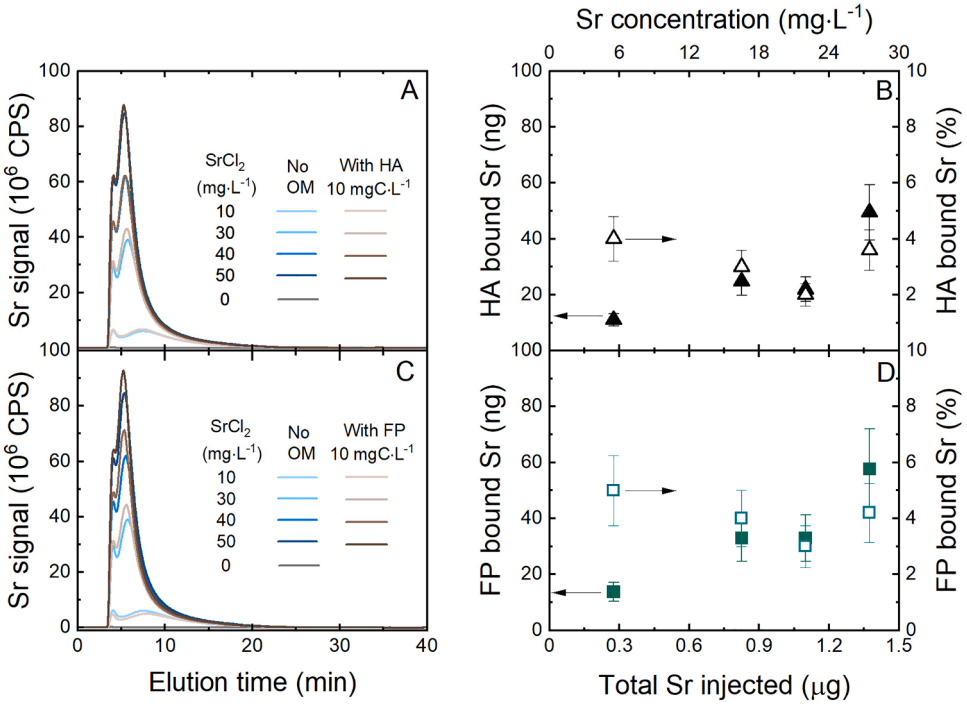

Fig. 9. Sr signal (in FFFF-ICP-MS) as a function of elution time at different Sr concentrations with and without HA (A) and FP (C); amount of Sr bound with HA (B) and FP (D) as a function of Sr injected mass or concentration. OM concentration was fixed at 10 mgC.L^{-1}.

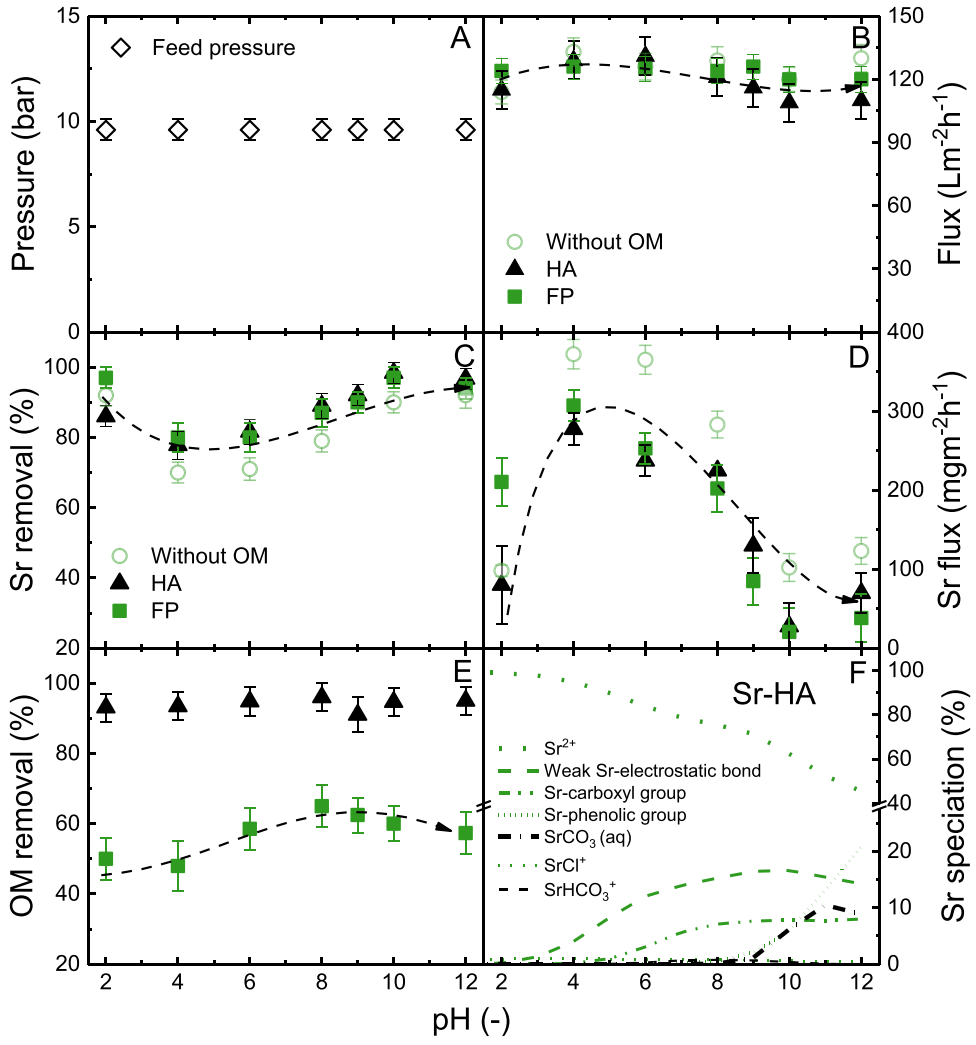

Fig. 10. (A) Feed pressure; (B) membrane steady-state flux; (C) Sr removal; (D) Sr flux; (E) OM removal and (F) Sr speciation with HA as a function of pH. NF270, 60 % recovery, 10 mgC.L^{-1} OM with 10 mg.L^{-1} $SrCl_2$, 10 mM NaCl and 1 mM $NaHCO_3$, 25 ± 1.

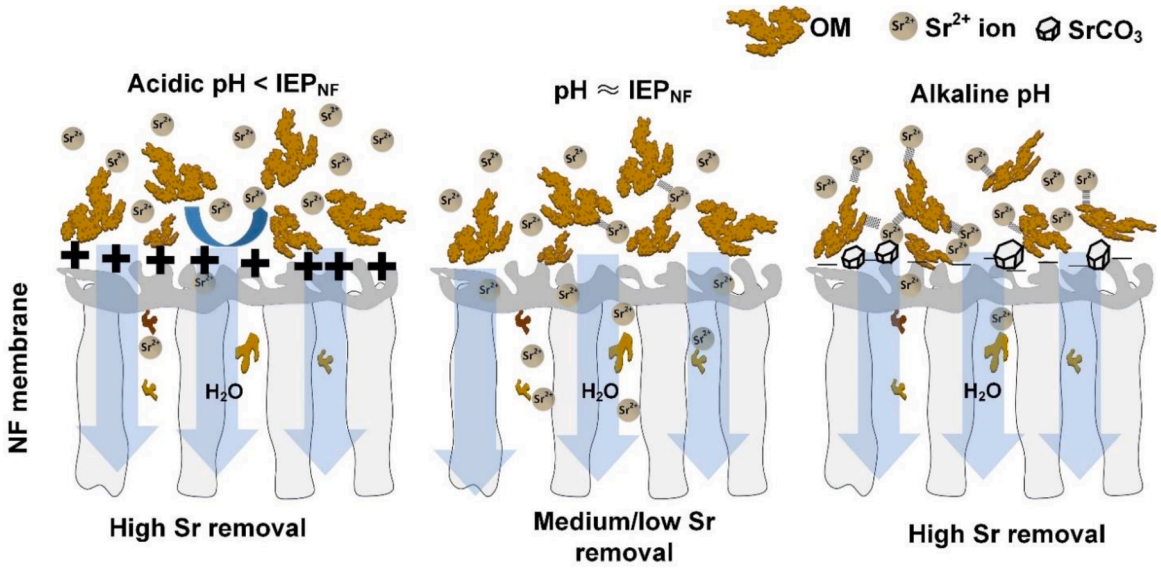

Fig. 11. Schematic of Sr removal mechanism with different pH in the presence of organic matter.

Sr-HA and Sr-FP binding were in a similar range, regardless of Sr concentration at 10 mgC.L^{-1} OM concentration. At those Sr and OM concentrations, where the OM/Sr ratio is lower than the critical OM/Sr ratio, the extent of Sr-HA and Sr-FP binding does not differ from each other. So, the extent of Sr-HA and Sr-FP complex formation is not a decisive factor for Sr retention when the OM/Sr ratio is low.

The surface charge of the membranes upon exposure to Sr-OM complex was measured to evaluate if the surface charge modification influences Sr retention. The results are shown in Figure S9. Zeta potential of NF270 with HA-Sr deposition becomes more negatively charged than that with FP-Sr deposition when increasing pH from 2 to 10. This observation verifies the second hypothesis that the HA-Sr complexes deposition made the membrane surface more negatively charged than FP-Sr deposition, thus facilitating the adsorption of Sr^{2+} ions so that the Sr removal with HA is higher than that with FP. This will be investigated further with speciation that is determined by solution pH.

3.6. Strontium removal by nanofiltration with pH variation

Variable feedwater pH affects the membrane surface charge, OM structure, and OM-Sr interactions and speciation, which is bound to affect the Sr removal by NF. Therefore, this section aims to investigate how the OM-Sr speciation affects the Sr removal. The NF membrane performance and Sr speciation (Visual MINTEQ simulation with NICA-Donnan model for humic acid) as a function of a wide range of pH (2-12) is presented in Fig. 10. As indicated above, Visual MINTEQ simulation with NICA-Donnan model cannot be performed for FP as the model consists of only humic acid and fulvic acid parameters. The comparative representation of the binding sites of HA and FP based on their phenolic and carboxylic acidity is shown in Figure S1.

Extreme acidic condition pH 2 caused high Sr removal (Fig. 10C). This is probably due to the enhanced electrostatic interaction between Sr^{2+} and membrane surface since the membrane charge becomes positive (see Figure S9) (Mouhoumed et al., 2014). The lowest Sr removal was observed at pH 4 and 6, presumably due to a weaker charge exclusion, when the NF membrane surface becomes uncharged or less negatively charged, see Figure S9 (Mouhoumed et al., 2014). Increasing pH from 6 to 12 enhanced Sr removal, most likely due to the enhanced Sr-OM binding and occurrence of $SrCO_3$ at high pH (see Fig. 10F).

To summarize findings, the potential Sr removal mechanisms with OM in different pH values are proposed and shown in Fig. 11. pH plays a more significant role in determining the Sr retention when compared to the other factors such as organic matter type and quantity. At acidic pHs, Sr^{2+} is electrostatically repelled from the membrane surface as a result of the positive charge of the membrane. The membrane charge diminishes at pH 4-6 and charge exclusion becomes minimal, leading to the lowest removal of Sr. Alkaline pH resulted in an increase in Sr removal, most likely because high pH promotes Sr-OM binding and also due to the likelihood of coprecipitation of carbonates of Sr (Bostick et al., 1994). Different OM types also influence Sr removal differently. For example, as observed in the case of HA and FP, the presence of HA induces more Sr removal than FP due to the three main mechanisms: i) formation of a higher amount of HA-Sr complex than FP-Sr complex leading to more retention of Sr with HA, ii) increase in negative surface charge of the membrane by the deposition of HA-Sr leading to higher adsorption of Sr^{2+}, iii) more deposition of HA-Sr complex leading to a pore size reduction of the membrane and consequently greater steric exclusion of Sr. Thus, the synergistic effects of multiple mechanisms facilitate the removal of Sr in the presence of organic matter (OM) in NF.

4. Conclusions

The objective of this study was to investigate the strontium removal mechanism with nanofiltration membranes in the presence of a broad range of organic matter types (10 types) and pH (2 – 12). This study confirms the enhancement of Sr removal by NF membranes in the presence of organic matter, as a function of pH, thus speciation, where solute-solute interactions play an important role in the Sr removal by NF membranes.

The presence of different OM types and an increase of OM concentration can enhance Sr removal by NF, which is due to the enhanced solute-solute interactions (OM-Sr binding/complexation). The nature of Sr removal in presence of OM highly depends on the type and thus characteristics of the OM, especially at high OM concentrations. At a critical OM/Sr ratio of 4 mgC.mg^{-1} for FP and 11 mgC.mg^{-1} for HA the Sr-OM binding and Sr removal acquires a breakthrough where no further enhancement is observed. High Sr^{2+} concentration reduces the Sr removal in presence of OM, which is likely due to the enhanced free Sr^{2+} ions' diffusion and convention through NF membranes. Extremely low pH (pH 2) enhanced Sr removal due to enhanced charge exclusion of Sr^{2+}; while very high pH (pH 10) enhanced Sr removal, possibly by enhancing Sr-OM binding.

By applying a very complex tool, coupled FFFF-ICP-MS, OM-cation interactions could be quantified and this enabled the elucidation and verification of the mechanism by which OM affects Sr removal in NF.

CRediT authorship contribution statement

Yang-Hui Cai: Writing – review & editing, Writing – original draft, Visualization, Validation, Methodology, Investigation, Formal analysis, Data curation, Conceptualization. **Akhil Gopalakrishnan:** Writing – review & editing, Writing – original draft, Visualization, Validation, Methodology, Investigation. **Qilin Dong:** Investigation, Data curation. **Andrea I. Schäfer:** Conceptualization, Methodology, Funding acquisition, Resources, Writing – review & editing.

Declaration of competing interest

The authors declare that they have no known competing financial interests or personal relationships that could have appeared to influence the work reported in this paper.

Data availability

Data will be made available on request.

Acknowledgements

The authors would like to thank China Scholarship Council (CSC) for granting a Ph.D. scholarship to Y.-H. Cai. Helmholtz Recruitment Initiative awarded to A. I. Schäfer for funding of IAMT. Both DuPont Water Solutions Co. and Hydranautics Co. are thanked for providing the nanofiltration membrane samples, NF270 and HYDRACoRe 50 LD, respectively. At IAMT, Timur Okkali helped with Sr filtration experiments at different pH without organic matter. Minh Nguyen helped with LC-OCD instruction of usage, calibration and discussions. Dr Youssef-Amine Boussouga helped with ICP-MS operation and calibration, scientific discussions and comments. Dr Thomas Luxbacher from Anton Paar is thanked for performing the challenging zeta potential measurements of NF membranes with different organic matter types and for the helpful comments and discussions. Prof Erwin Klumpp (FZ Jülich, Germany) inspired the work on FFFF coupling methodology, while the BMBF IGSTC project CANDECT financed the instrument.

Supporting information

The supporting information includes: (1) characteristics of organic matter types; (2) feed solution composition for experiments; (3) zeta potential of chosen NF membranes as a function of pH; (4) detailed filtration protocol; (5) optimization of FFFF-ICP-MS coupling and

calibrations; (6) FFFF-ICP-MS protocol; (7) ICP-MS calibration and effect of OM types and OM concentration; (8) calibration of TOC analyser and LC-OCD; (9) the critical ratio of OM and Sr concentrations; (10) speciation of strontium-humic acid interactions; (11) error analysis; (12) role of organic fractions on strontium and organic matter removal (13) flux performance with OM concentration; (14) NF fouling with the variation of Sr and OM quantity.

Supplementary materials

Supplementary material associated with this article can be found, in the online version, at doi:10.1016/j.watres.2024.121241.

References

Adusei-Gyamfi, J., Ouddane, B., Rietveld, L., Cornard, J.P., Criquet, J., 2019. Natural organic matter-cations complexation and its impact on water treatment: a critical review. Water Res. 160, 130–147.

Al-Rashdi, B.A.M., Johnson, D.J., Hilal, N., 2013. Removal of heavy metal ions by nanofiltration. Desalination 315, 2–17.

Alasonati, E., Stolpe, B., Benincasa, M.A., Hassellöv, M., Slaveykova, V.I., 2006. Asymmetrical flow field flow fractionation-multidetection system as a tool for studying Metal-Alginate interactions. Environ. Chem. 3, 192–198.

Asymmetric flow field flow fractionation, in: Light scattering, size exclusion chromatography and asymmetric flow field flow fractionation, 2011, pp. 259–305.

Atkins, P., Paula, J.d., 2009. Chemical equilibrium: electrochemistry. In: Atkins, P., Paula, J.d. (Eds.), Elements of Physical Chemistry. OUP Oxford.

Baalousha, M., Stolpe, B., Lead, J.R., 2011. Flow field-flow fractionation for the analysis and characterization of natural colloids and manufactured nanoparticles in environmental systems: a critical review. J. Chromatogr. A 1218, 4078–4103.

Baken, S., Degryse, F., Verheyen, L., Merckx, R., Smolders, E., 2011. Metal complexation properties of freshwater dissolved organic matter are explained by its aromaticity and by anthropogenic ligands. Environ. Sci. Technol. 45, 2584–2590.

Bendixen, N., Losert, S., Adlhart, C., Lattuada, M., Ulrich, A., 2014. Membrane–particle interactions in an asymmetric flow field flow fractionation channel studied with titanium dioxide nanoparticles. J. Chromatogr. A 1334, 92–100.

Boguta, P., Sokołowska, Z., 2013. Interactions of humic acids with metals. Acta Agrophys. Monograph. 2, 1–113.

Boiteau, R.M., Fitzsimmons, J.N., Repeta, D.J., Boyle, E.A., 2013. Detection of iron ligands in seawater and marine cyanobacteria cultures by high-performance liquid chromatography–inductively coupled plasma-mass spectrometry. Anal. Chem. 85, 4357–4362.

Bolea, E., Laborda, F., Castillo, J.R., 2010. Metal associations to microparticles, nanocolloids and macromolecules in compost leachates: size characterization by asymmetrical flow field-flow fractionation coupled to ICP-MS. Anal. Chim. Acta 661, 206–214.

Borggaard, O.K., Holm, P.E., Strobel, B.W., 2019. Potential of dissolved organic matter (DOM) to extract As, Cd, Co, Cr, Cu, Ni, Pb and Zn from polluted soils: a review. Geoderma 343, 235–246.

Bostick, D.A., Arnold, W.D., Jr., Burgess, M.W., Strontium removal from caustic carbonate waste solutions using carrier coprecipitation, in, United States, 1994, pp. 12.

Boussouga, Y.A., Mohankumar, M.B., Gopalakrishnan, A., Welle, A., Schäfer, A.I., 2021. Removal of arsenic(III) via nanofiltration: contribution of organic matter interactions. Water Res. 201, 117315.

Boussouga, Y.A., Okkali, T., Luxbacher, T., Schäfer, A.I., 2023. Chromium (III) and chromium (VI) removal and organic matter interaction with nanofiltration. Sci. Total Environ. 885, 163695.

Braghetta, A., DiGiano, F.A., Ball, W.P., 1997. Nanoflitration of natural organic matter: pH and ionic strength effects. J. Environ. Eng. 123, 628–641.

Cai, Y.H., Yang, X.J., Schäfer, A.I., 2020a. Removal of naturally occurring strontium by nanofiltration/reverse osmosis from groundwater. Membranes (Basel) 10, 321.

Cai, Y.H., Yang, X.J., Schäfer, A.I., 2020b. Removal of naturally occurring strontium by nanofiltration/reverse osmosis from groundwater. Membranes 10, 321.

Cai, Y.H., Gopalakrishnan, A., Deshmukh, K.P., Schafer, A.I., 2022. Renewable energy powered membrane technology: implications of adhesive interaction between membrane and organic matter on spontaneous osmotic backwash cleaning. Water Res. 221, 118752.

Chegrouche, S., Mellah, A., Barkat, M., 2009. Removal of strontium from aqueous solutions by adsorption onto activated carbon: kinetic and thermodynamic studies. Desalination 235, 306–318.

Chen, D., Zhao, X., Li, F., 2014. Treatment of low level radioactive wastewater by means of NF process. Nucl. Eng. Des. 278, 249–254.

Chen, L., Bian, X., Lu, X., 2018a. Removal of strontium from simulated low-level radioactive wastewater by nanofiltration. Water Sci. Technol. 78, 1733–1740.

Childress, A.E., Elimelech, M., 1996. Effect of solution chemistry on the surface charge of polymeric reverse osmosis and nanofiltration membranes. J. Membr. Sci. 119, 253–268.

Childress, A.E., Elimelech, M., 2000. Relating nanofiltration membrane performance to membrane charge (electrokinetic) characteristics. Environ. Sci. Technol. 34, 3710–3716.

Claveranne-Lamolère, C., Lespes, G., Dubascoux, S., Aupiais, J., Pointurier, F., Potin-Gautier, M., 2009. Colloidal transport of uranium in soil: size fractionation and characterization by field-flow fractionation–multi-detection. J. Chromatogr. A 1216, 9113–9119.

Cuss, C.W., Grant-Weaver, I., Shotyk, W., 2017. AF4-ICPMS with the 300Da membrane to resolve metal-bearing "colloids" < 1 kDa: optimization, fractogram deconvolution, and advanced quality control. Anal. Chem. 89, 8027–8035.

Delpla, I., Jung, A.V., Baures, E., Clement, M., Thomas, O., 2009. Impacts of climate change on surface water quality in relation to drinking water production. Environ. Int. 35, 1225–1233.

Dewey, C., Kaplan, D.I., Fendorf, S., Boiteau, R.M., 2023. Quantitative separation of unknown organic–metal complexes by liquid chromatography–inductively coupled plasma-mass spectrometry. Anal. Chem. 95, 7960–7967.

Ding, S., Yang, Y., Huang, H., Liu, H., Hou, L.A., 2015. Effects of feed solution chemistry on low pressure reverse osmosis filtration of cesium and strontium. J. Hazard Mater. 294, 27–34.

Dorsey, A.F., Fransen, M.E., Diamond, G.L., Amata, R.J., 2004. Toxicological Profile For Strontium. ATSDR, Atlanta, Georgia, p. 445.

Dublet, G., Worms, I., Frutschi, M., Brown, A., Zünd, G.C., Bartova, B., Slaveykova, V.I., Bernier-Latmani, R., 2019. Colloidal size and redox state of uranium species in the porewater of a pristine mountain wetland. Environ. Sci. Technol. 53, 9361–9369.

Felmy, A.R., Dixon, D.A., Rustad, J.R., Mason, M.J., Onishi, L.M., 1998. The hydrolysis and carbonate complexation of strontium and calcium in aqueous solution. Use of molecular modeling calculations in the development of aqueous thermodynamic models. J. Chem. Thermodyn. 30, 1103–1120.

Flury, M., Gimmi, T.F., 2002. 6.2 Solute diffusion. Methods of Soil Analysis. Soil Science Society of America, Inc., pp. 1323–1351

Gaubert, E., Barnier, H., Maurel, A., Foos, J., Guy, A., Bardot, C., Lemaire, M., 1997. Selective strontium removal from a sodium nitrate aqueous medium by nanofiltration - complexation. Sep. Sci. Technol. 32, 585–597.

Gopalakrishnan, A., Bouby, M., Schäfer, A.I., 2023a. Membrane-organic solute interactions in asymmetric flow field flow fractionation: interplay of hydrodynamic and electrostatic forces. Sci. Total Environ. 855, 158891.

Gopalakrishnan, A., Bouby, M., Schafer, A.I., 2023b. Membrane-organic solute interactions in asymmetric flow field flow fractionation: interplay of hydrodynamic and electrostatic forces. Sci. Total Environ. 855, 158891.

Gutierrez, M., Fuentes, H.R., 1991. Competitive adsorption of cesium, cobalt and strontium in conditioned clayey soil suspensions. J. Environ. Radioact. 13, 271–282.

Hartland, A., Fairchild, I.J., Lead, J.R., Zhang, H., Baalousha, M., 2011. Size, speciation and lability of NOM–metal complexes in hyperalkaline cave dripwater. Geochim. Cosmochim. Acta 75, 7533–7551.

Health Canada, 2018. Strontium in drinking water- guideline technical document for public consultation. In: Proceedings of the Canada Federal-Provincial-Territorial Committee on Drinking Water.

Hofer, T.S., Randolf, B.R., Rode, B.M., 2006. Sr(II) in water: a labile hydrate with a highly mobile structure. J. Phys. Chem. B 110, 20409–20417.

Hu, X., Qu, C., Han, Y., Chen, W., Huang, Q., 2022. Elevated temperature altered the binding sequence of Cd with DOM in arable soils. Chemosphere 288, 132572.

Huber, S.A., Balz, A., Abert, M., Pronk, W., 2011. Characterisation of aquatic humic and non-humic matter with size-exclusion chromatography – organic carbon detection – organic nitrogen detection (LC-OCD-OND). Water Res. 45, 879–885.

Hydranutics, HYDRACoRe10 and 50 LD series datasheet, in, Oceanside, CA 92058, USA, 2018.

Imbrogno, A., Schäfer, A.I., 2019. Comparative study of nanofiltration membrane characterization devices of different dimension and configuration (cross flow and dead end). J. Membr. Sci. 585, 67–80.

Imbrogno, A., Tiraferri, A., Abbenante, S., Weyand, S., Schwaiger, R., Luxbacher, T., Schäfer, A.I., 2018. Organic fouling control through magnetic ion exchange-nanofiltration (MIEX-NF) in water treatment. J. Memb. Sci. 549, 474–485.

Kamaraj, R., Vasudevan, S., 2015. Evaluation of electrocoagulation process for the removal of strontium and cesium from aqueous solution. Chem. Eng. Res. Des. 93, 522–530.

Kavurt, U.B., Marioli, M., Kok, W.T., Stamatialis, D., 2015. Membranes for separation of biomacromolecules and bioparticles via flow field-flow fractionation. J. Chem. Technol. Biotechnol 90, 11–18.

Keuth, U., Leinenbach, A., Beck, H.P., Wagner, H., 1998. Separation and characterization of humic acids and metal humates by electrophoretic methods. Electrophoresis 19, 1091–1096.

Khandare, A.L., Validandi, V., Rajendran, A., Singh, T.G., Thingnganing, L., Kurella, S., Nagaraju, R., Dheeravath, S., Vaddi, N., Kommu, S., Maddela, Y., 2020. Health risk assessment of heavy metals and strontium in groundwater used for drinking and cooking in 58 villages of Prakasam district, Andhra Pradesh, India. Environ. Geochem. Health 42, 3675–3701.

Kim, D.H., Moon, J., Cho, J., 2005. Identification of natural organic matter (NOM) transport behavior near the membrane surface using flow field-flow-fractionation (fl-FFF) micro channel. J. Water Supply: Res. Technol.-Aqua 54, 249–259.

Kinniburgh, D.G., Milne, C.J., Benedetti, M.F., Pinheiro, J.P., Filius, J., Koopal, L.K., Riemsdijk, W.H.V., 1996. Metal ion binding by humic acid: application of the NICA-Donnan model. Environ. Sci. Technol. 30, 1687–1698.

Kinniburgh, D.G., van Riemsdijk, W.H., Koopal, L.K., Borkovec, M., Benedetti, M.F., Avena, M.J., 1999. Ion binding to natural organic matter: competition, heterogeneity, stoichiometry and thermodynamic consistency. Colloids Surf., A 151, 147–166.

Koopal, L.K., Saito, T., Pinheiro, J.P., Riemsdijk, W.H.v., 2005. Ion binding to natural organic matter: general considerations and the NICA–Donnan model. Colloids Surf. A Physicochem. Eng. Asp. 265, 40–54.

Latorre, M., Herbello-Hermelo, P., Peña-Farfal, C., Neira, Y., Bermejo-Barrera, P., Moreda-Piñeiro, A., 2019. Size exclusion chromatography – inductively coupled plasma – mass spectrometry for determining metal-low molecular weight compound complexes in natural wines. Talanta 195, 558–565.
Lauchnor, E.G., Schultz, L.N., Bugni, S., Mitchell, A.C., Cunningham, A.B., Gerlach, R., 2013. Bacterially induced calcium carbonate precipitation and strontium coprecipitation in a porous media flow system. Environ. Sci. Technol. 47, 1557–1564.
Lechtenfeld, O.J., Koch, B.P., Geibert, W., Ludwichowski, K.U., Kattner, G., 2011. Inorganics in organics: quantification of organic phosphorus and sulfur and trace element speciation in natural organic matter using HPLC-ICPMS. Anal. Chem. 83, 8968–8974.
Li, X., Cao, Z., Du, Y., Zhang, Y., Wang, J., Ma, X., Hu, P., Luo, Y., Wu, L., 2024. Multi-metal contaminant mobilizations by natural colloids and nanoparticles in paddy soils during reduction and reoxidation. J. Hazard. Mater. 461, 132684.
Lipczynska-Kochany, E., 2018. Effect of climate change on humic substances and associated impacts on the quality of surface water and groundwater: a review. Sci. Total Environ. 640-641, 1548–1565.
Listiarini, K., Sun, D.D., Leckie, J.O., 2009. Organic fouling of nanofiltration membranes: evaluating the effects of humic acid, calcium, alum coagulant and their combinations on the specific cake resistance. J. Membr. Sci. 332, 56–62.
Liu, M., Han, X., Liu, C.Q., Guo, L., Ding, H., Lang, Y., 2021. Differences in the spectroscopic characteristics of wetland dissolved organic matter binding with Fe3+, Cu2+, Cd2+, Cr3+ and Zn2+,. Sci. Total Environ 800, 149476.
Luo, J., Wan, Y., 2013. Effects of pH and salt on nanofiltration—A critical review. J. Memb. Sci. 438, 18–28.
Moradi, G., Bol, R., Trbojevic, L., Missong, A., Mörchen, R., Fuentes, B., May, S.M., Lehndorff, E., Klumpp, E., 2020. Contrasting depth distribution of colloid-associated phosphorus in the active and abandoned sections of an alluvial fan in a hyper-arid region of the Atacama Desert. Glob. Planet Change 185, 103090.
Mostofa, K.M.G., Liu, C.-q., Feng, X., Yoshioka, T., Vione, D., Pan, X., Wu, F., Complexation of dissolved organic matter with trace metal Ions in natural waters, in: K.M.G. Mostofa, T. Yoshioka, A. Mottaleb et al. (Eds.) Photobiogeochemistry of Organic matter: Principles and Practices in Water Environments, Springer Berlin Heidelberg, Berlin, Heidelberg, 2013, pp. 769–849.
Mouhoumed, E.I., Szymczyk, A., Schäfer, A., Paugam, Lydie, La, Y.H., 2014. Physico-chemical characterization of polyamide NF/RO membranes: insight from streaming current measurements. J. Memb. Sci. 461, 130–138.
Musgrove, M., 2021. The occurrence and distribution of strontium in U.S. groundwater. Appl. Geochem. 126, 104867.
Nair, R.R., Protasova, E., Strand, S., Bilstad, T., 2018. Implementation of Spiegler–Kedem and steric hindrance pore models for analyzing nanofiltration membrane performance for smart water production. Membranes 8, 78.
Neale, P.A., Schäfer, A.I., 2012. Quantification of solute–solute interactions in steroidal hormone removal by ultrafiltration membranes. Sep. Purif. Technol. 90, 31–38.
Neubauer, E., Köhler, S.J., von der Kammer, F., Laudon, H., Hofmann, T., 2013. Effect of pH and stream order on iron and arsenic speciation in boreal catchments. Environ. Sci. Technol. 47, 7120–7128.
Newcombe, H.B., 1957. Magnitude of biological hazard from strontium-90. Science 126, 549–551.
Nguyen, M.N., Hérvas-Martínez, R., Schäfer, A.I., 2021. Organic matter interference with steroid hormone removal by single-walled carbon nanotubes – ultrafiltration composite membrane. Water Res. 199, 117148.
Nifant'eva, T.I., Burba, P., Fedorova, O., Shkinev, V.M., Spivakov, B.Y., 2001. Ultrafiltration and determination of Zn– and Cu–humic substances complexes stability constants. Talanta 53, 1127–1131.
O'Donnell, A.J., Lytle, D.A., Harmon, S., Vu, K., Chait, H., Dionysiou, D.D., 2016. Removal of strontium from drinking water by conventional treatment and lime softening in bench-scale studies. Water Res. 103, 319–333.
Oatley-Radcliffe, D.L., Walters, M., Ainscough, T.J., Williams, P.M., Mohammad, A.W., Hilal, N., 2017. Nanofiltration membranes and processes: a review of research trends over the past decade. J. Water Process Eng. 19, 164–171.
Park, B., Ghoreishian, S.M., Kim, Y., Park, B.J., Kang, S.M., Huh, Y.S., 2021. Dual-functional micro-adsorbents: application for simultaneous adsorption of cesium and strontium. Chemosphere 263, 128266.
Pathak, P., Srivastava, R.R., Keceli, G., Mishra, S., 2020. Assessment of the alkaline earth metals (Ca, Sr, Ba) and their associated health impacts. In: Pathak, P., Gupta, D.K. (Eds.), Strontium Contamination in the Environment, The Handbook of Environmental Chemistry 88. Springer Nature Switzerland AG, pp. 227–231.
Peng, H., Yao, F., Xiong, S., Wu, Z., Niu, G., Lu, T., 2021. Strontium in public drinking water and associated public health risks in Chinese cities. Environ. Sci. Pollut. Res. Int. 28, 23048–23059.
Pesavento, M., Alberti, G., Biesuz, R., 2009. Analytical methods for determination of free metal ion concentration, labile species fraction and metal complexation capacity of environmental waters: a review. Anal. Chim. Acta 631, 129–141.
Pornwilard, M.M., Siripinyanond, A., 2014. Field-flow fractionation with inductively coupled plasma mass spectrometry: past, present, and future. J. Anal. At. Spectrom. 29, 1739–1752.
Pothier, M.P., Lenoble, V., Garnier, C., Misson, B., Rentmeister, C., Poulain, A.J., 2020. Dissolved organic matter controls of arsenic bioavailability to bacteria. Sci. Total Environ. 716, 137118.
Powell, B.A., Miller, T., Kaplan, D.I., 2015. On the influence of ionic strength on radium and strontium sorption to sandy loam soils. JSC Acad. Sci. 13, 13–18.
Rana, D., Matsuura, T., Kassim, M.A., Ismail, A.F., 2013. Radioactive decontamination of water by membrane processes — A review. Desalination 321, 77–92.
Rard, J.A., Miller, D.G., 1982. Mutual diffusion coefficients of $SrCl_2$–H_2O and CsCl—H_2O at 25°C from Rayleigh interferometry. J. Chem. Soc. 78, 887–896. Faraday Transactions 1: Physical Chemistry in Condensed Phases.
Rathgeb, A., Causon, T., Krachler, R., Hann, S., 2016. Determination of size-dependent metal distribution in dissolved organic matter by SEC-UV/VIS-ICP-MS with special focus on changes in seawater. Electrophoresis 37, 1063–1071.
Ritson, J.P., Graham, N.J., Templeton, M.R., Clark, J.M., Gough, R., Freeman, C., 2014. The impact of climate change on the treatability of dissolved organic matter (DOM) in upland water supplies: a UK perspective. Sci. Total Environ. 473-474, 714–730.
Rottmann, L., Heumann, K.G., 1994. Determination of heavy metal interactions with dissolved organic materials in natural aquatic systems by coupling a high-performance liquid chromatography system with an inductively coupled plasma mass spectrometer. Anal. Chem. 66, 3709–3715.
Schaep, J., Van der Bruggen, B., Vandecasteele, C., Wilms, D., 1998. Retention mechanisms in nanofiltration. In: Pawłowski, L., Gonzales, M.A., Dudzińska, M.R., Lacy, W.J. (Eds.), Chemistry For the Protection of the Environment 3. Springer US, Boston, MA, pp. 117–125.
Shim, Y., Lee, H.J., Lee, S., Moon, S.H., Cho, J., 2002. Effects of natural organic matter and ionic species on membrane surface charge. Environ. Sci. Technol. 36, 3864–3871.
Sillanpää, M.E.T., 2015. Natural Organic Matter in Water: Characterization and Treatment Methods, 1st ed. Elsevier, Butterworth-Heinemann, Finland.
Skougstad, M.W., Horr, C.A., 1963. Occurrence and distribution of strontium in natural water. In: Geological Survey, Superintendent of Documents, 25. U.S. Government Printing Office, Washington, pp. 55–97. D.G.
Stolpe, B., Guo, L., Shiller, A.M., Aiken, G.R., 2013. Abundance, size distributions and trace-element binding of organic and iron-rich nanocolloids in Alaskan rivers, as revealed by field-flow fractionation and ICP-MS. Geochim. Cosmochim. Acta 105, 221–239.
Suarez, D.L., 1996. Beryllium, magnesium, calcium, strontium and barium. Methods of Soil Analysis Part 3-Chemical Methods. Soil Science Society of America and American Society of Agronomy, p. 576.
Tang, C.Y., Kwon, Y.N., Leckie, J.O., 2007. Fouling of reverse osmosis and nanofiltration membranes by humic acid—Effects of solution composition and hydrodynamic conditions. J. Memb. Sci. 290, 86–94.
Tipping, E., Hurley, M.A., 1992. A unifying model of cation binding by humic substances. Geochim. Cosmochim. Acta 56, 3627–3641.
US-EPA, 2014. In: Agency, E.P. (Ed.), Announcement of Preliminary Regulatory Determinations for Contaminants on the Third Drinking Water Contaminant Candidate List. US-EPA, Washington, DC.
US-EPA, 2018. 2018 Edition of the Drinking Water Standards and Health Advisories Tables. US-EPA, Washington, DC.
Wadekar, S.S., Vidic, R.D., 2018. Insights into the rejection of barium and strontium by nanofiltration membrane from experimental and modeling analysis. J. Memb. Sci. 564, 742–752.
World Health Organization, Guidelines for drinking-water quality, in, 2017.
Worms, I.A.M., Al-Gorani Szigeti, Z., Dubascoux, S., Lespes, G., Traber, J., Sigg, L., Slaveykova, V.I., 2010. Colloidal organic matter from wastewater treatment plant effluents: characterization and role in metal distribution. Water Res. 44, 340–350.
Worms, I.A.M., Chmiel, H.E., Traber, J., Tofield-Pasche, N., Slaveykova, V.I., 2019. Dissolved organic matter and associated trace metal dynamics from river to lake, under ice-covered and ice-free conditions. Environ. Sci. Technol. 53, 14134–14143.
Wu, F., Evans, D., Dillon, P., Schiff, S., 2004. Molecular size distribution characteristics of the metal–DOM complexes in stream waters by high-performance size-exclusion chromatography (HPSEC) and high-resolution inductively coupled plasma mass spectrometry (ICP-MS). J. Anal. At. Spectrom. 19, 979–983.
Xu, H., Yan, Z., Cai, H., Yu, G., Yang, L., Jiang, H., 2013. Heterogeneity in metal binding by individual fluorescent components in a eutrophic algae-rich lake. Ecotoxicol. Environ. Saf. 98, 266–272.
Xu, F., Yao, Y., Alvarez, P.J.J., Li, Q., Fu, H., Yin, D., Zhu, D., Qu, X., 2019. Specific ion effects on the aggregation behavior of aquatic natural organic matter. J. Colloid Interface Sci. 556, 734–742.
Yao, X., Su, C., Fan, T., Ren, H., Luo, F., 2022. Investigating the binding properties between strontium and dissolved organic matter under the influence of pH and Ca^{2+} in a typical Karst Area, China. Land 11, 1376.
Zhao, S., Chen, Y., Wu, G., Li, J., Ren, Y., Duan, X., 2023. Investigation on nanofiltration membrane fouling behaviour of cation-induced apam in strontium-bearing mine water. J. Environ. Chem. Eng. 11, 110940.